Journal of Colloid and Interface Science 585 (2021) 400–407

Contents lists available at ScienceDirect

Journal of Colloid and Interface Science

journal homepage: www.elsevier.com/locate/jcis

Regular Article

Rapid removal of organic pollutants by a novel persulfate/brochantite system: Mechanism and implication

Wanyue Dong [a,b,1], Tao Cai [c,1], Yutang Liu [a,b,*], Longlu Wang [d], Hui Chen [a,b], Wengao Zeng [a,b], Juan Li [a,b], Wenlu Li [a,b]

[a] College of Environmental Science and Engineering, Hunan University, Lushan South Road, Yuelu District, Changsha 410082, PR China
[b] Key Laboratory of Environmental Biology and Pollution Control (Hunan University), Ministry of Education, Lushan South Road, Yuelu District, Changsha 410082, PR China
[c] School of Resource & Environment and Safety Engineering, University of South China, Hengyang 421001, PR China
[d] College of Electronic and Optical Engineering & College of Microelectronics, Nanjing University of Posts and Telecommunications, Nanjing 210023, PR China

GRAPHICAL ABSTRACT

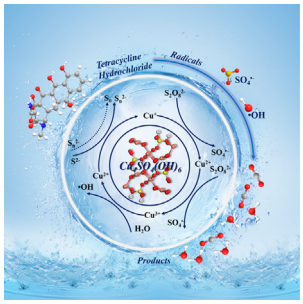

ARTICLE INFO

Article history:
Received 4 September 2020
Revised 7 November 2020
Accepted 26 November 2020

Keywords:
In situ chemical oxidation
Persulfates
Brochantite
Tetracycline hydrochloride

ABSTRACT

Using natural minerals as persulfate activators can develop effective and economical in situ chemical oxidation technology for environmental remediation. Yet, few natural minerals can provide a high activation efficiency. Here, we demonstrate that brochantite ($Cu_4SO_4(OH)_6$), a natural mineral, can be used as a persulfate activator for the rapid degradation of tetracycline hydrochloride (TC-H). Approximately 70% of TC-H was removed in $Cu_4SO_4(OH)_6$/PDS within 5 min, which much higher than that of Cu_3P (61.99%), CuO (29.75%), CNT (25.83%), Fe_2O_3, (14.48%) and MnO_2 (9.76%). Experiments and theoretical calculations suggested that surface copper acts as active sites induce the production of free radicals. The synergistic effect of Cu/S promotes the cycle between Cu^+/Cu^{2+}. Sulfate radicals and hydroxyl radicals are the main reactive oxygen species that are responsible for the rapid removal of TC-H. The findings of this work show a novel persulfate/brochantite system and provide useful information for the environmental remediation.

1. Introduction

Persulfates (including peroxymonosulfate (PMS) and peroxydisulfate (PDS)) are commonly used for in situ chemical oxidation (ISCO) to purify the contaminated water bodies because they are not only relatively cheap and stable than hydrogen peroxide (H_2O_2) but also can work in a wide pH range.[1,2] Persulfate can be activated to produce sulfate radicals ($SO_4^{\bullet-}$), hydroxyl radicals (•OH)) and other active substances, thereby degrading most organic contaminants rapidly. Ultraviolet[3], base[4], heat[5,6], transition metal ions,[7,8] metal oxides,[9–11] metal sulfide,[12] metal phosphide,[13] graphitic carbon nitride[14,15] and carbon materials,[16,17] have been reported to be effective in persulfate

* Corresponding author at: College of Environmental Science and Engineering, Hunan University, Lushan South Road, Yuelu District, Changsha 410082, PR China.
E-mail address: yt_liu@hnu.edu.cn (Y. Liu).
[1] These authors contributed equally to this work.

https://doi.org/10.1016/j.jcis.2020.11.106
0021-9797/

activation process. Recently, it has also been reported that natural metal nanoparticles[18] cobalt or iron-based minerals[19] and organic compounds[20] are capable of activating persulfate to degrade contaminants. Understanding the interaction between these natural substances and persulfate could provide some useful and fundamental information for finding or designing new catalysts. However, current research is mainly focused on metal oxide-based minerals, and little is known about the effects of other natural substances, especially some hydroxysulfate based minerals, on the activation of persulfate.

Copper hydroxysulfate ($Cu_4SO_4(OH)_6$), namely brochantite, is a common mineral and the corrosion product of copper metals and alloys.[21] Additionally, it is also used as fungicides or spray for seed treatment or control of plant fungal diseases.[22] Several previous studies showed that brochantite can be utilized for enzyme immobilization[23] and synthesize copper oxide.[24] Few reports have been devoted to investigated its intrinsic catalytic performance yet. Recently, Xiao et al.[25] showed that $Cu_4SO_4(OH)_6$ exhibited good catalytic activity for catalytic H_2O_2 oxidation, and Cu^{2+} was speculated to be the catalytic active species in this process. Similarly, Huang et al.[26] investigated the effects of the morphology of $Cu_4SO_4(OH)_6$ on catalytic performance toward the degradation of phenol with the aid of H_2O_2. They found that $Cu_4SO_4(OH)_6$ with more mesopores facilitated the diffusion of phenol, leading to better catalytic activity. However, detailed research on the catalytic mechanism of $Cu_4SO_4(OH)_6$ based ISCO process is still lacking. It is unclear whether $Cu_4SO_4(OH)_6$ can react with persulfate and what reaction mechanism would be involved in this process. Recent works showed that in addition to traditional free radical pathways, a nonradical pathway was involved in the process of persulfate activation by either mediated electron transfer or singlet oxygenation.[27,28] Therefore, there is an urgent need to systematically study the catalytic behavior and mechanism of $Cu_4SO_4(OH)_6$/persulfate system. More importantly, because brochantite is widely distributed in the natural environment, it is of great significance to study the interaction between $Cu_4SO_4(OH)_6$ and persulfate and the effects on the degradation of contaminants.

This work is primarily focus on following issues: (i) can persulfate be activated by $Cu_4SO_4(OH)_6$; (ii) can $Cu_4SO_4(OH)_6$ be used as a high-efficient catalyst for persulfate to degrade pollutants; and (iii) what is the underlying mechanism of this catalytic process. To answer the above questions, $Cu_4SO_4(OH)_6$ and PDS were employed as the catalyst and oxidant to degrade a model pollutant, tetracycline hydrochloride (TC-H). The catalytic performance, kinetics, and mechanism were thoroughly investigated by detailed experimental techniques and density function theory (DFT) calculation. Its advantages over other common catalysts were also investigated in aspects of catalytic performance. Effects of initial pH, temperature, inorganic ion, catalysts dosage, and oxidants dosage on the PDS activation process were further investigated. Additionally, the stability of $Cu_4SO_4(OH)_6$ was also evaluated.

2. Experimental section

2.1. Chemical Agents and Characterization method are provided in Supporting Information (Text S1-2).

3. Materials preparation

NaOH solution (15 ml, 0.1 M) was added into $CuSO_4$ solution (20 ml. 0.1 M), and then L-ascorbic acid solution (5 ml, 0.1 M) was injected rapidly and kept stirring for 30 min. Finally, $Na_2S{\cdot}9H_2O$ (2 ml, 0.1 M) was added into above mixed solution and kept stirring until the aqueous color became blackish green. After washing and drying, $Cu_4SO_4(OH)_6$ sample was obtained. Several metal oxides (i.e., MnO_2, Fe_2O_3, Cu_2O, and CuO) and carbon nanotube were purchased from Aladdin. CuS was obtained by direct reaction of $CuSO_4$ and $Na_2S{\cdot}9H_2O$ at room temperature (RT). Cu_3P was prepared according to the previous report.[13]

3.1. Catalytic experiments

The degradation experiment was performed in a 50 ml beaker at RT. 5 mg of catalysts was suspended in the reaction solution (50 ml, 20 mg/L TC-H). Then, the PDS stock solution ($K_2S_2O_8$ from Aladdin) was added into above reaction solution to trigger the degradation reaction. At a given interval time, 1 ml of suspension was withdrawn and filtered through 0.45 μm filter membrane for further analysis. The concentrations of TC-H were measured by the optical absorption at 357 nm with a UV–vis spectrophotometer. PDS concentration was tested by potassium iodide method (Text S3).[29] pH tested by a pH meter (FE28, Mettler Toledo). The production of radicals was detected by electron paramagnetic resonance (JES FA200) (Text S4). Dissolved copper was tested by an inductively coupled plasma emission spectrometer (ICP-OES, Agilent 725 ICP-OES).

3.2. Density function theory (DFT) calculation

All structure optimization calculations were performed using Materials Studio (MS) program with Cambridge serial total energy package (CASTEP) code.[30] GGA-PBE0 functional formalism was applied with normconserving pseudopotentials. The Monkhorst–Pack scheme was used to construct the k-point meshes for Brillouin zone sampling.

4. Results and discussions

4.1. Catalytic activity of $Cu_4SO_4(OH)_6$

The as-prepared $Cu_4SO_4(OH)_6$ was mainly in irregular bulk form with a diameter of 0.2 ~ 2 μm (Figure S1). The XRD patterns (Figure S2a) were consistent with the monoclinic structure of $Cu_4SO_4(OH)_6$ samples (PDF# 43–1458).[26] Besides, a small amount of CuS (PDF# 06–0464) impurities appeared, which may be originate from the preparation process. The XPS survey spectra (Figure S2b) showed that the sample contained only Cu, O, S, and C elements and no other impurities appeared.

The catalytic activity of as-prepared $Cu_4SO_4(OH)_6$ to activate PDS for the degradation of TC-H was studied. As shown in Fig. 1a, PDS alone had almost no activity for the degradation of TC-H, and $Cu_4SO_4(OH)_6$ itself only had very limited absorption toward TC-H. In contrast, approximately 80% of TC-H was removed in $Cu_4SO_4(OH)_6$/PDS with 4 min, indicating that efficient PDS activation by $Cu_4SO_4(OH)_6$ was achieved. Additionally, under the same experimental conditions, only 20% of TC-H was removed in CuS/PDS within 4 min (Figure S3). Considering the low content of CuS impurities in the as-prepared catalyst, the TC-H degradation caused by impurities can be ignored. Therefore, the above results showed that the entire reaction process was dominated by $Cu_4SO_4(OH)_6$-based heterogeneous catalysis. The removal efficiency of TC-H by PDS oxidation using $Cu_4SO_4(OH)_6$, CuO, Cu_3P, Fe_2O_3, MnO_2, and CNT as catalysts were further evaluated (Fig. 1b). Among these catalysts, the removal efficiency of TC-H was in the order of $Cu_4SO_4(OH)_6$ (69.98%) > Cu_3P (61.99%) > CuS (30.31%) > CuO (29.75%) > CNT (25.83%) > Fe_2O_3 (14.48%) > MnO_2 (9.76%). The result clearly showed that $Cu_4SO_4(OH)_6$ was a promising catalyst for PDS activation. It displayed the highest activity among these common catalysts under our experimental conditions.

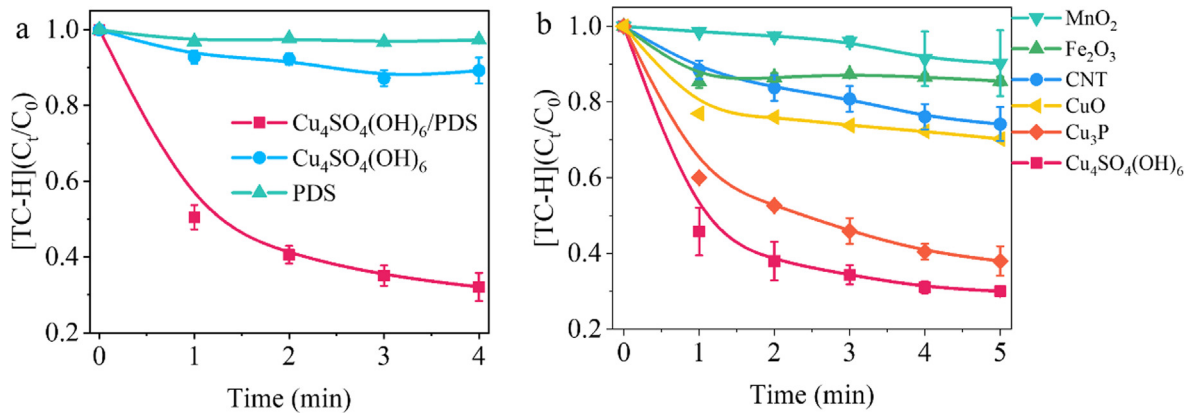

Fig. 1. The evaluation of catalytic activity of $Cu_4SO_4(OH)_6$. (a) The degradation of TC-H in $Cu_4SO_4(OH)_6$/PDS system. (b) The degradation of TC-H in different system. Experimental conditions: [TC-H] = 20 mg/L, [PDS] = 0.45 mM, [Catalysts] = 0.1 g/L.

To the best of our knowledge, this is the first study about the high activity $Cu_4SO_4(OH)_6$ in heterogeneous catalytic PDS activation. Further research was performed to investigate the kinetics, mechanism, stability, and some influence factors in $Cu_4SO_4(OH)_6$/PDS system, which could be beneficial to evaluate its practical application and provide some fundamental information.

4.2. Kinetic model

The overall reaction rate equation can be expressed in equation (eq) 1 or eq 2, where k represents the apparent reaction rate constant; a and b represent reaction order. Firstly, we supposed that the initial concentration of $Cu_4SO_4(OH)_6$ in $Cu_4SO_4(OH)_6$/PDS system is $[Cu_4SO_4(OH)_6]_0$, the concentration of PDS is $[PDS]_0$, thus the reaction rate at t = 0 can be described as eq 3 or eq 4.

$$v = -(dc/dt) = k[Cu_4SO_4(OH)_6]^a[PDS]^b \quad (1)$$

$$-lg(dc/dt) = lgk + alg[Cu_4SO_4(OH)_6] + blg[PDS] \quad (2)$$

$$v = -(dc/dt) = k[Cu_4SO_4(OH)_6]_0^a[PDS]_0^b \quad (3)$$

$$-lg(dc/dt) = lgk + alg[Cu_4SO_4(OH)_6]_0 + blg[PDS]_0 \quad (4)$$

Secondly, a sequence of $Cu_4SO_4(OH)_6$ with different dosages was used in the TC-H solution, but the concentrations of PDS was fixed. Then, the degradation curve of TC-H versus (vs) time was recorded. The equation of this curve can be acquired, where t and c represent the independent variable and dependent variable, respectively. The equation derivative can be expressed to -lg(dc/dt) at different $[Cu_4SO_4(OH)_6]_0$ values at t = 0. Since the dosages of PDS is fixed, $lgk + blg[PDS]_0$ is constant. Therefore, -lg(dc/dt) has a linear relationship with $[Cu_4SO_4(OH)_6]_0$. Using -lg(dc/dt) as the dependent variable and $[Cu_4SO_4(OH)_6]_0$ as the independent variable, an linear curve can be obtained, where the slope is a, and the intercept is $lgk + blg[PDS]_0$. Similarly, the data for b, and $lgk + alg[Cu_4SO_4(OH)_6]_0$ can also be figured out. Finally, the value of k can be calculated and the overall reaction rate equation can be established. The details of these calculations can be found in Fig. 2 and TableS1-2.

As shown in Fig. 2a, plotting -lg(dc/dt) vs $lg([Cu_4SO_4(OH)_6]_0)$ output a straight line with a slope approximating 0.081 and intercept approximating 1.086 (eq 5), indicating that a was 0.081 and that $lgk + blg[PDS]_0$ was equal to 1.086. Similarly, we can also acquire that b was 0.904 and that $lgk + alg[Cu_4SO_4(OH)_6]_0$ was equal to 1.240 (Fig. 2b and eq 6). The total reaction rate constant k was calculated to be 22.91 by the combination of eq 5–6. Therefore, under our experimental conditions, the total reaction rate equation can be expressed as eq 7. The overall reaction order (a + b) is between zero- and first-order kinetics.

$$-lg(dc/dt) = 1.086 + 0.081 \times lg\,[Cu_4SO_4(OH)_6]_0 \quad (5)$$

$$-lg(dc/dt) = 1.240 + 0.904 \times lg\,[PDS]_0 \quad (6)$$

$$v = 22.91[Cu_4SO_4(OH)_6]^{0.081}[PDS]^{0.904} \quad (7)$$

4.3. Reaction mechanism

4.3.1. Identification of active substances

To explore the reaction mechanism of $Cu_4SO_4(OH)_6$/PDS system, the generation of reactive oxygen species (ROSs) were identified by electron paramagnetic resonance (EPR) technology and ROSs quenching experiment. 5,5-dimethyl pyrroline-oxide (DMPO) was used as the spin trapping reagent to detect the production of $SO_4^{\bullet-}$ and •OH.[31] As shown in Fig. 3a, no EPR signals can be detected in PDS alone, indicating that un-activation PDS cannot produce radicals. However, the obvious EPR signals of DMPO-$SO_4^{\bullet-}$ and DMPO-•OH were appeared in $Cu_4SO_4(OH)_6$/PDS system, suggesting that both $SO_4^{\bullet-}$ and •OH were generated. To further identify the role of ROSs, the removal of TC-H by $Cu_4SO_4(OH)_6$/PDS system was carried out in the presence of different sacrificial agents, where ethanol (EtOH), isopropanol (IPA), and L-histidine were used as the scavengers for $SO_4^{\bullet-}$, •OH[32], and singlet oxygen ($^1O_2$).[33] When EtOH, IPA and L-histidine added into $Cu_4SO_4(OH)_6$/PDS system, the remove efficiency of TC-H obviously decreased (Fig. 3b), suggesting that $SO_4^{\bullet-}$,•OH, and $^1O_2$ play important roles during the degradation process.

It should be pointed out that using L-histidine or azide as $^1O_2$ scavengers may cause misinterpretation on persulfate activation processes because these substances can directly react with persulfate.[27] Actually, after carefully analyzing the reaction process, we believed that $^1O_2$ could not result in an obvious TC-H degradation under our experimental conditions. On the one hand, PDS itself can be decomposed to produce a large amount of $^1O_2$. If $^1O_2$ is the main active substance, then the un-activated PDS should also have a certain catalytic activity for the degradation of TC-H, which is inconsistent with the experimental results. On the other hand, the CNT/PDS system, a well-known $^1O_2$ generation system, was employed to degrade TC-H and compared with $Cu_4SO_4(OH)_6$/PDS system. Figure S4 showed that CNT/PDS system had no obvious catalytic activity for the degradation of TC-H, but had a certain adsorptive property, which was contrary to the $Cu_4SO_4(OH)_6$/PDS system. This result showed that the reaction mechanism of the two systems was different and $^1O_2$ played a negligible role in the degradation process of TC-H. Additionally, nonradicals mechanism through direct

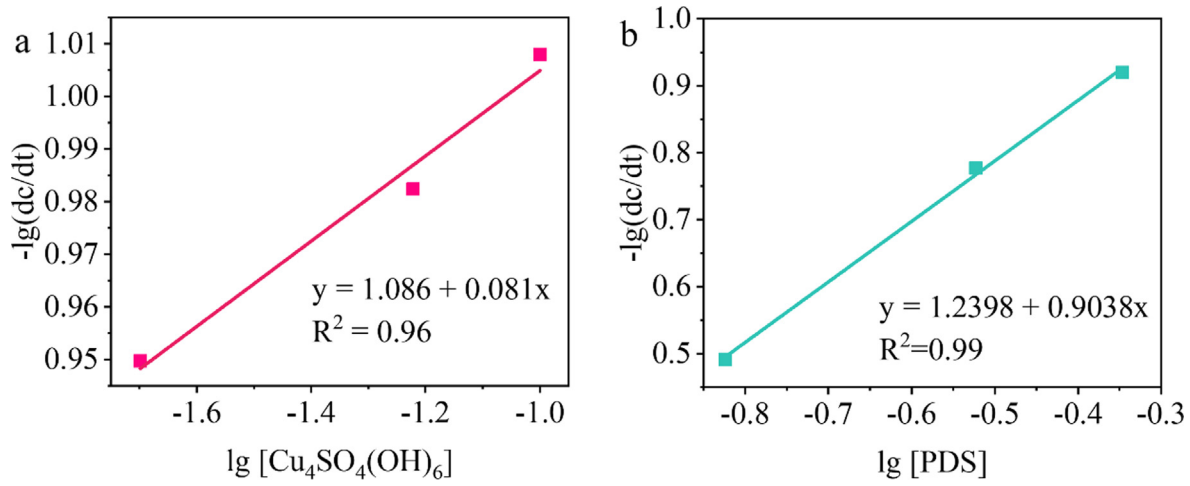

Fig. 2. Apparent kinetic equations. The fitting line between -lg(dc/dt) and lg[$Cu_4SO_4(OH)_6$]$_0$. The fitting line between -lg(dc/dt) and lg[PDS]$_0$.

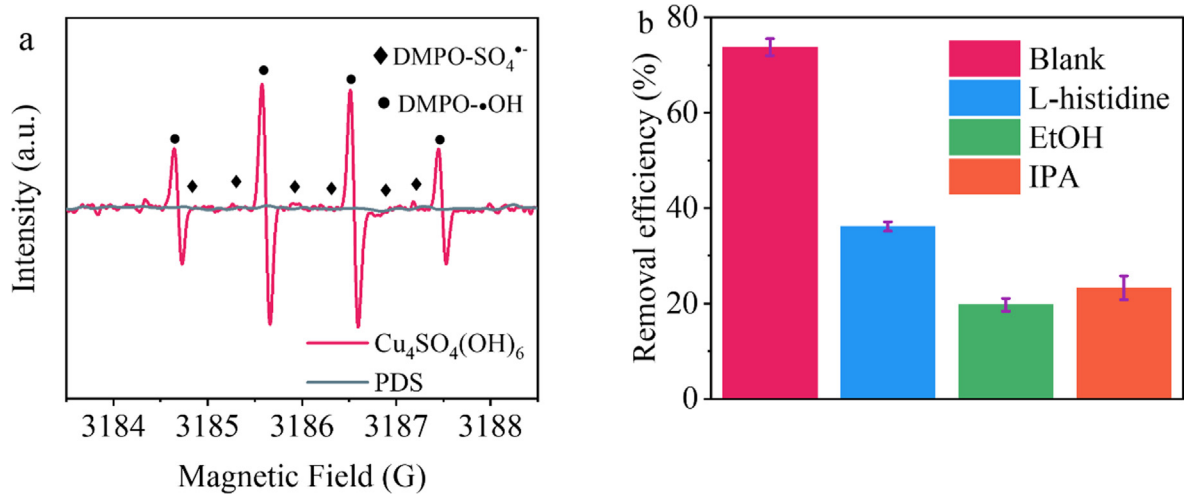

Fig. 3. Identification of active substances. (a) EPR spectra for the test of free radicals. (b) The degradation of TC-H by $Cu_4SO_4(OH)_6$/PDS system in the presence of different radical sacrifice agents.

electron transfer from pollutants to PDS/Catalyst (e.g., CuO[34]) also can be excluded because PDS can be efficiently decomposed by $Cu_4SO_4(OH)_6$ regardless of with or without TC-H (Figure S5). To sum up, the activation mechanism of PDS by $Cu_4SO_4(OH)_6$ may be dominated by a radical-based reaction.

4.3.2. Identification of the active site

A recent study showed that some functional groups such as –C=O, –OH, and –COOH may be catalytic active sites in PDS activation.[35] Duan et al. used 1,2-dihydroxybenzene to mimic –OH group to probe the role of –OH group.[16] They revealed that –OH group was not the main active sites for PDS activation. Our experimental results also demonstrated this conclusion. The XPS spectra of O 1 s peak are shown in Figure S6. The main peak at 531.8 eV and 533.2 eV were attributed to the –OH component and the O in adsorbed H_2O.[36] After the reaction, there was almost no change in the O 1 s peak, indicating that the –OH component may not participate in the activation process. Therefore, the –OH group in $Cu_4SO_4(OH)_6$ was not the main active site in PDS activation.

Interestingly, The Cu 2p peak undergoes slightly variations after reaction (Fig. 4a). For the fresh $Cu_4SO_4(OH)_6$, the Cu 2p spectra included two main peaks, Cu $2p_{3/2}$ and Cu $2p_{1/2}$, respectively. The peaks can be deconvoluted and each peak can be fitted to two peaks (approximately 932.0 eV and 934.5 eV for Cu $2p_{3/2}$, 951.8 eV, and 954.2 eV for Cu $2p_{1/2}$).[37] The peaks located at 932.0 eV and 951.8 eV corresponding to Cu^+, while the peaks located at 934.5 eV and 954.2 eV corresponding to Cu^{2+}. Because $Cu_4SO_4(OH)_6$ involved two types of Cu–O bonds, namely Cu–O–Cu bond and Cu–O–SO_3, representing a combination of Cu_2O and $CuSO_4$ type contributions.[37,38] After the reaction, the percentage of Cu^+ component versus Cu^{2+} component decreased, indicating that the oxidation of surface Cu^+ occurs during the reaction process. Given that there was no drastic change in shape of Cu 2p peak after the reaction, indicating that there were still many Cu^+ and Cu^{2+} species on the surface of $Cu_4SO_4(OH)_6$, revealing the good recycle of Cu^{2+}/Cu^+ in $Cu_4SO_4(OH)_6$/PDS system. Fig. 4b showed the S 2p spectra of $Cu_4SO_4(OH)_6$. The peaks located at 161.79 eV, 163.01 eV, and 164.04 eV were assigned to S^{2-}, S_n^{2-} and S_0, respectively.[12] Meanwhile, it was observed the proportion of $S^{2-}$and S_n^{2-} decreased from 49.68% and 22.31% to 41.4%, and 17.13%, respectively, while the percentage of S_0 increased from 28.01% to 41.45%, indicating that $S^{2-}$and S_n^{2-} species may be oxidized to S_0 during the activation process. Thus, both surface Cu and S are involved in this reaction and may exist a synergistic effect. This situation was similar to that of $CuFeS_2$, where S^{2-} facilitated the

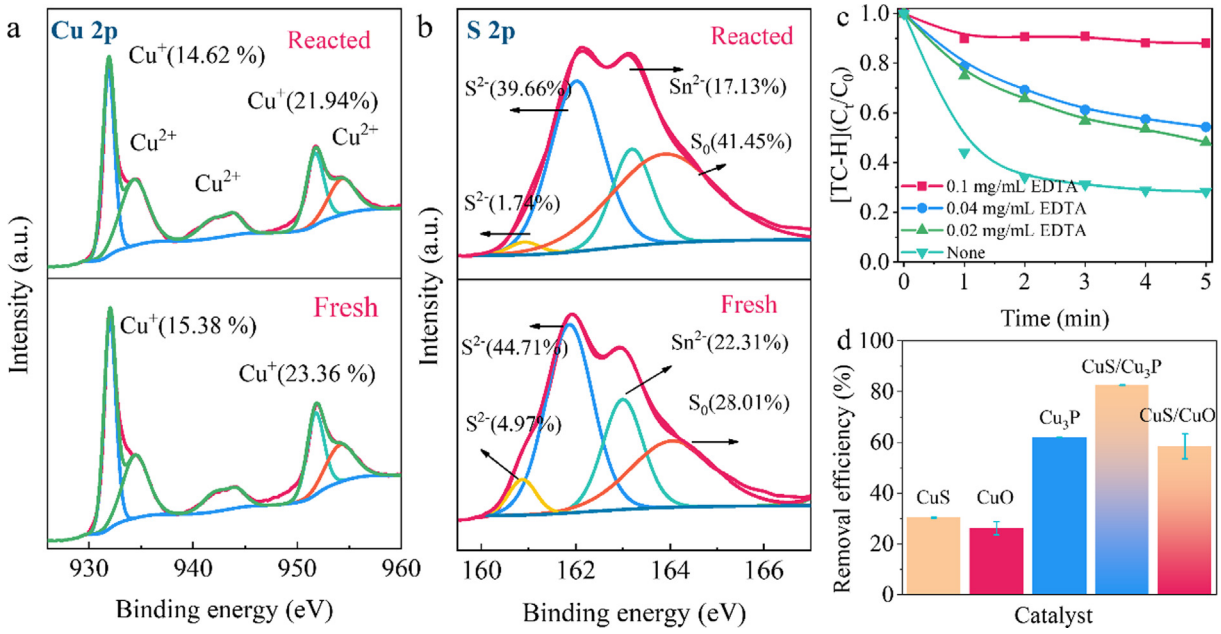

Fig. 4. Identification of active sites. (a) The variation of XPS spectra of Cu 2p before and after reaction. (b) The variation of XPS spectra of S 2p before and after reaction. (c) The degradation of TC-H by $Cu_4SO_4(OH)_6$/PDS system in the presence of EDTA. (d) TC-H degradation by PDS oxidation with various catalysts and different combinations. Experimental conditions: [TC-H] = 20 mg/L, [PDS] = 0.45 mM, [Catalysts] = 0.1 g/L.

cycling of Cu^{2+}/Cu^{+} and Fe^{3+}/Fe^{2+}.[39] Therefore, a possible synergy reaction mechanism was proposed (eq 8–14).

$$\equiv Cu^{+} + S_2O_8^{2-} \rightarrow \equiv Cu^{2+} + SO_4^{2-} + SO_4^{\bullet -} \quad (8)$$

$$\equiv Cu^{2+} + S_2O_8^{2-} \rightarrow \equiv Cu^{3+} + SO_4^{2-} + SO_4^{\bullet -} \quad (9)$$

$$\equiv Cu^{3+} + H_2O \rightarrow \equiv Cu^{2+} + \bullet OH + H^{+} \quad (10)$$

$$2 \equiv S^{2-} + 2 \equiv Cu^{2+} \rightarrow 2 \equiv Cu^{+} + \equiv S_n^{2-} \quad (11)$$

$$\equiv S_n^{2-} + 2 \equiv Cu^{2+} \rightarrow 2 \equiv Cu^{+} + \equiv S_0 \quad (12)$$

$$SO_4^{\bullet -} + H_2O \rightarrow \bullet OH + SO_4^{2-} + H^{+} \quad (13)$$

$$SO_4^{\bullet -}/\bullet OH + \text{TC-H} \rightarrow \text{Products} \quad (14)$$

To further identify the role of Cu^{+}/Cu^{2+}, ethylene diamine tetraacetic acid (EDTA), a chelating agent, was added into the $Cu_4SO_4(OH)_6$/PDS system. The carboxyl groups of EDTA can coordinate with surface Cu to form the metal-carboxyl complex,[40] which could cover active sites for PDS activation, thereby lowing TC-H degradation efficiency. As shown in Fig. 4c, the removal efficiency of TC-H was suppressed gradually as the EDTA concentration increased, implying that surface Cu was involved in the PDS activation. A series of combinations of CuS, CuO, and Cu_3P were employed to investigate the role of S for PDS activation (Fig. 4d). The removal efficiency of TC-H within 5 min was in the order of Cu_3P/CuS (82.5%) > Cu_3P (62%) > CuO/CuS (58.4%) > CuS (30.3%) > CuO (26.2%). Theoretically, the removal efficiency of the Cu_3P/CuS should be between those of Cu_3P and CuS. However, the Cu_3P/CuS displayed better catalytic activity than both pure Cu_3P and pure CuS. Similarly, CuO/CuS also showed better than CuO or CuS alone. These results suggesting that a synergistic effect between $\equiv S^{2-}$ and $\equiv Cu^{+}$ or $\equiv Cu^{2+}$ occurred during the PDS activation. $\equiv S^{2-}$ could keep recycling of $\equiv Cu^{2+}/Cu^{+}$ by donating an electron to regenerate $\equiv$Cu sites. In conclusion, the above results and discussions demonstrated that $\equiv$Cu in $Cu_4SO_4(OH)_6$ was the active site for PDS activation, and $\equiv S^{2-}$ can maintain the recycle of $\equiv Cu^{2+}/Cu^{+}$. The hydroxy group played a negligible role in the PDS activation process.

4.3.3. Theoretical calculation

DFT calculation was carried out to further uncover the mystery of the reaction mechanism in the $Cu_4SO_4(OH)_6$/PDS system. The structure models of $Cu_4SO_4(OH)_6$ are displayed in Fig. 5a. To study the bonding behavior between the atoms, the electron density difference map was investigated (Fig. 5b) and a plane containing Cu, S, and O atoms was chosen. As shown in Fig. 5c, electron mainly accumulated around the O atoms and consumed around the Cu atoms, indicating that positively charged Cu atoms had greater potential for the adsorption of PDS through electrostatic attraction. To further reveal the situation of electron transmission between $Cu_4SO_4(OH)_6$ and PDS, the electron density difference map was performed at $Cu_4SO_4(OH)_6$-PDS interface (Fig. 5d). In $Cu_4SO_4(OH)_6$/PDS system electron mainly accumulated around the O atoms of PDS adjacent to Cu atoms of $Cu_4SO_4(OH)_6$ (Fig. 5e), suggesting that electron tend to transfer from Cu atoms of $Cu_4SO_4(OH)_6$ to O atoms of PDS (Fig. 5f). This electron transfer process is also confirmed by electrochemical analysis. As observed in Figure S7, when PDS was added Na_2SO_4 solution, an obvious current signal was generated on the $Cu_4SO_4(OH)_6$ electrode, indicating that $Cu_4SO_4(OH)_6$ donated electrons to PDS, leading to a sudden increase in current. Therefore, Cu atoms as adsorption and active sites donated electrons to PDS to generate free radicals. The theoretical calculation results are consistent with the previous experimental results.

4.4. Influence factors

4.4.1. Influence of pH.

Figure S8a showed the variation of TC-H removal efficiency at different pH. The $Cu_4SO_4(OH)_6$/PDS displayed the highest TC-H removal efficiency at pH 7. The removal efficiency decreased under acidic or alkaline conditions. Under acidic conditions, the removal rate of the TC-H is related to the adsorption of $Cu_4SO_4(OH)_6$ toward TC-H. As the pH decreases, the adsorption of TC-H by $Cu_4SO_4(OH)_6$ decreased. However, $Cu_4SO_4(OH)_6$ can be "etched" in the alkaline environment (eq 15).[41] Thus, the catalytic performance was

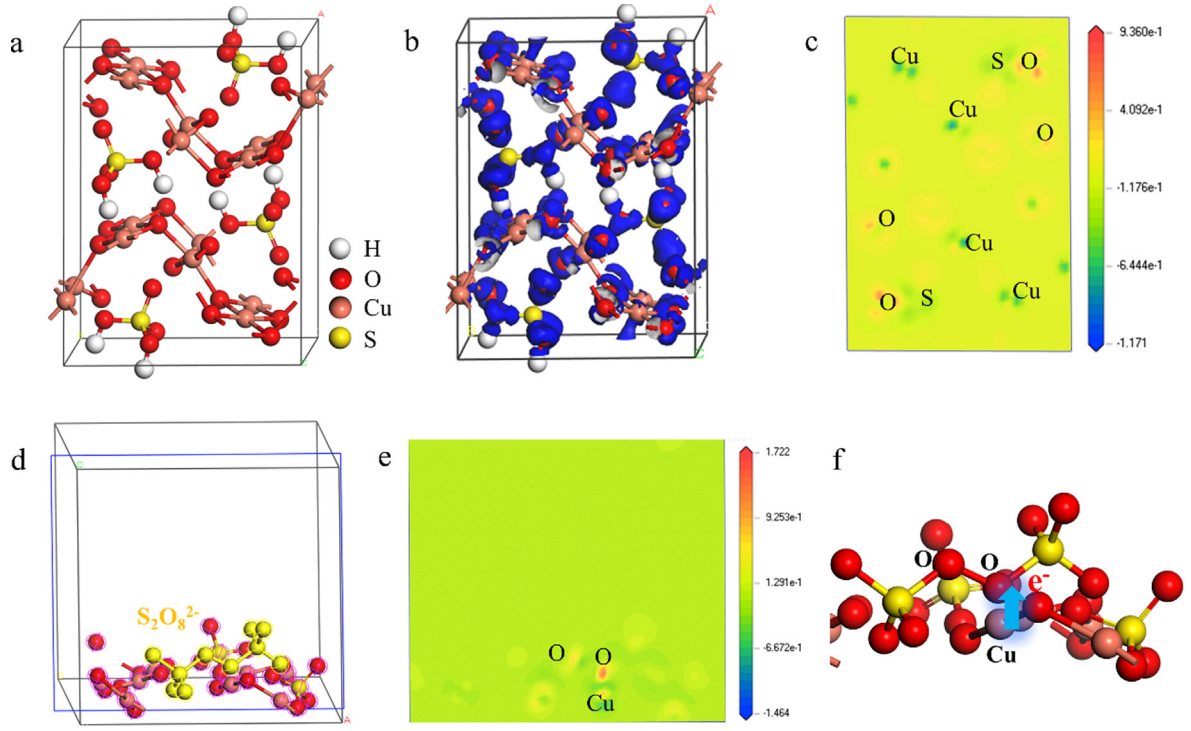

Fig. 5. Density function theory calculation studies of $Cu_4SO_4(OH)_6$. (a) The structure models of $Cu_4SO_4(OH)_6$. (b) The calculation of electron-density difference of $Cu_4SO_4(OH)_6$. (c) The electron-density difference map of $Cu_4SO_4(OH)_6$. (d) The calculation of electron-density difference at $Cu_4SO_4(OH)_6$-PDS interface. (e) The electron-density difference map of $Cu_4SO_4(OH)_6$/PDS. (f) Schematic illustration of electron transfer at $Cu_4SO_4(OH)_6$-PDS interface.

greatly decreased under alkaline conditions due to the damage of the catalyst.

$$Cu_4SO_4(OH)_6 + 2OH^- \rightarrow 4Cu(OH)_2 + SO_4^{2-} \quad (15)$$

4.4.2. Influence of natural organic matter and inorganic ion

The degradation of organic contaminants induced by radicals in actual water bodies is commonly inhibited by some natural organic matter and inorganic ion.[14,33] Therefore, humic acid (HA), chloride ions (Cl^-), and bicarbonate ions (HCO_3^-) were chosen as representative species to investigated influences on TC-H degradation in $Cu_4SO_4(OH)_6$/PDS system. As shown in Figure S8b, the degradation of TC-H was distinctly suppressed in presence of HA, Cl^-, or HCO_3^-, indicating that side reactions between these specials and radicals have occurred. This result further proved that the entire reaction is a radical reaction. HCO_3^- and Cl^- can scavenge active radicals to produce less active oxidative species, resulting in the suppression of the degradation (eq 16–21).[42] HA caused an obvious inhibition of the degradation of TC-H because it is a powerful competitor.

$$SO_4^{\bullet-} + Cl^- \rightarrow SO_4^{2-} + Cl^- \quad (16)$$

$$\bullet OH + Cl^- \rightarrow ClOH^{\bullet-} \quad (17)$$

$$Cl^- + H_2O \rightarrow ClOH^{\bullet-} \quad (18)$$

$$ClOH^{\bullet-} + Cl^- \rightarrow Cl_2^- \quad (19)$$

$$SO_4^{\bullet-} + HCO_3^- \rightarrow CO_3^{\bullet-} + SO_4^{2-} + H^+ \quad (20)$$

$$\bullet OH + HCO_3^- \rightarrow CO_3^{\bullet-} + H_2O \quad (21)$$

4.4.3. Influence of the dosage of $Cu_4SO_4(OH)_6$ and PDS

As the dosage of $Cu_4SO_4(OH)_6$ increases from 1 mg to 10 mg, the removal efficiency of TC-H was also improved (Figure S 9a). The improved TC-H removal efficiency can be attributed to the more active sites from higher $Cu_4SO_4(OH)_6$ dosage. Similarly, the removal efficiency increased with the increase of PDS concentration. In particular, the maximum removal efficiency of TC-H was achieved under the PDS concentration of 0.45 mM (Figure S9b). Higher doses of PDS could accelerate the production of free radicals, thereby improving the degradation of TC-H. However, excessive PDS would consume reactive oxidation species, which are harmful to the catalytic process.[43] Additionally, the influence of reactive temperature on the degradation of TC-H was also investigated. As observed in Figure S10, elevated temperature from 25 ℃ – 45 ℃ slightly enhanced the degradation of TC-H in the $Cu_4SO_4(OH)_6$/PDS system.

4.5. Stability

The stability of $Cu_4SO_4(OH)_6$ during the catalytic process was evaluated by multiple cycling experiments. Experimental results showed that $Cu_4SO_4(OH)_6$ can keep good catalytic activity in three cycles without a serious recession (Figure S11a). The XRD pattern of $Cu_4SO_4(OH)_6$ after the cycling experiment almost keep the same with fresh $Cu_4SO_4(OH)_6$, which also demonstrated that $Cu_4SO_4(OH)_6$ is stable during this catalytic process (Figure S11b). These results proved that $Cu_4SO_4(OH)_6$ can be used as a promising heterogeneous PDS activator for environmental remediation.

5. Conclusion

The activation of PDS has been intensively investigated and employed for the ISCO of contaminated groundwater. $Cu_4SO_4(OH)_6$ is a common mineral and as the product of corrosion of copper metal and alloys, which is widely distributed in the natural environment. The findings of this work revealed a novel $Cu_4SO_4(OH)_6$/PDS system for efficient degradation of organic pollutants, which provide useful information for developing PDS based ISCO for environmental cleaning. It was proved that $Cu_4SO_4(OH)_6$ displayed the highest catalytic performance among several common catalysts.

Experimental results showed that ≡Cu in $Cu_4SO_4(OH)_6$ was the active site for PDS activation, and $\equiv S^{2-}$ can maintain the recycle of $\equiv Cu^{2+}/Cu^{+}$. After three cycling tests, it also maintains good catalytic activity, which indicates that $Cu_4SO_4(OH)_6$ may be a promising catalyst for PDS activation. However, further studies are needed to identify the intermediate products of TC-H degradation to better understand the degradation mechanism and evaluate its practical application. The situation of PDS activation by PMS for the degradation of organic pollutants is also worthy of further study.

CRediT authorship contribution statement

Wanyue Dong: Methodology, Data curation, Writing - original draft. **Tao Cai:** Conceptualization, Writing - review & editing. **Yutang Liu:** Supervision, Project administration, Funding acquisition, Writing - review & editing. **Longlu Wang:** . **Hui Chen:** Formal analysis. **Wengao Zeng:** Validation, Data curation. **Juan Li:** Validation, Data curation. **Wenlu Li:** Formal analysis.

Declaration of Competing Interest

The authors declare that they have no known competing financial interests or personal relationships that could have appeared to influence the work reported in this paper.

Acknowledgements

This work was supported by the National Natural Science Foundation of China (51872089 and 51672077), the Hunan Provincial Natural Science Foundation of China (2017JJ2026) and the Key Laboratory of Jiangxi Province for Persistent Pollutants Control and resources Recycle (Nanchang hangkong University) (ES201880051). The authors thank National supercomputing center in Changsha for supporting this work.

Appendix A. Supplementary material

Chemical agents, characterization method, Figure S1-11 and Table S1-2 to this article can be found online at https://doi.org/10.1016/j.jcis.2020.11.106.

References

[1] S. Wacławek, H.V. Lutze, K. Grübel, V.V.T. Padil, M. Černík, D.D. Dionysiou, Chemistry of persulfates in water and wastewater treatment: A review, Chem. Eng. J. 330 (2017) 44–62.
[2] B.C. Hodges, E.L. Cates, J.H. Kim, Challenges and prospects of advanced oxidation water treatment processes using catalytic nanomaterials, Nat. Nanotechnol. 13 (2018) 642–650.
[3] C. Luo, J. Ma, J. Jiang, Y. Liu, Y. Song, Y. Yang, Y. Guan, D. Wu, Simulation and comparative study on the oxidation kinetics of atrazine by UV/H(2)O(2), UV/HSO(5)(-) and UV/S(2)O(8)(2)(-), Water Res. 80 (2015) 99–108.
[4] Y. Zhou, Y. Xiang, Y. He, Y. Yang, J. Zhang, L. Luo, H. Peng, C. Dai, F. Zhu, L. Tang, Applications and factors influencing of the persulfate-based advanced oxidation processes for the remediation of groundwater and soil contaminated with organic compounds, J. Hazard. Mater. 359 (2018) 396–407.
[5] M. Zhang, X. Chen, H. Zhou, M. Murugananthan, Y. Zhang, Degradation of p-nitrophenol by heat and metal ions co-activated persulfate, Chem. Eng. J. 264 (2015) 39–47.
[6] X. Duan, S. Indrawirawan, J. Kang, W. Tian, H. Zhang, X. Duan, X. Zhou, H. Sun, S. Wang, Synergy of carbocatalytic and heat activation of persulfate for evolution of reactive radicals toward metal-free oxidation, Catal Today (2019).
[7] J. Chen, X. Zhou, P. Sun, Y. Zhang, C.H. Huang, Complexation Enhances Cu(II)-Activated Peroxydisulfate: A Novel Activation Mechanism and Cu(III) Contribution, Environ. Sci. Technol. (2019).
[8] Z. Wang, J. Jiang, S. Pang, Y. Zhou, C. Guan, Y. Gao, J. Li, Y. Yang, W. Qiu, C. Jiang, Is Sulfate Radical Really Generated from Peroxydisulfate Activated by Iron(II) for Environmental Decontamination?, Environ. Sci. Technol. (2018).
[9] H. Wu, X. Xu, L. Shi, Y. Yin, L.C. Zhang, Z. Wu, X. Duan, S. Wang, H. Sun, Manganese oxide integrated catalytic ceramic membrane for degradation of organic pollutants using sulfate radicals, Water Res. 167 (2019) 115110.
[10] J. Lim, Y. Yang, M.R. Hoffmann, Activation of Peroxymonosulfate by Oxygen Vacancies-Enriched Cobalt-Doped Black TiO2 Nanotubes for the Removal of Organic Pollutants, Environ. Sci. Technol. (2019).
[11] Y. Feng, D. Wu, Y. Deng, T. Zhang, K. Shih, Sulfate Radical-Mediated Degradation of Sulfadiazine by CuFeO2 Rhombohedral Crystal-Catalyzed Peroxymonosulfate: Synergistic Effects and Mechanisms, Environ. Sci. Technol. 50 (2016) 3119–3127.
[12] J. Peng, X. Lu, X. Jiang, Y. Zhang, Q. Chen, B. Lai, G. Yao, Degradation of atrazine by persulfate activation with copper sulfide (CuS): Kinetics study, degradation pathways and mechanism, Chem. Eng. J. 354 (2018) 740–752.
[13] C. Alexopoulou, A. Petala, Z. Frontistis, C. Drivas, S. Kennou, D.I. Kondarides, D. Mantzavinos, Copper phosphide and persulfate salt: A novel catalytic system for the degradation of aqueous phase micro-contaminants, Appl. Catal. B 244 (2019) 178–187.
[14] B. Sun, W. Ma, N. Wang, P. Xu, L. Zhang, B. Wang, H. Zhao, K.A. Lin, Y. Du, Polyaniline: A New Metal-Free Catalyst for Peroxymonosulfate Activation with Highly Efficient and Durable Removal of Organic Pollutants, Environ. Sci. Technol. (2019).
[15] H. Li, C. Shan, B. Pan, Fe(III)-Doped g-C3N4 Mediated Peroxymonosulfate Activation for Selective Degradation of Phenolic Compounds via High-Valent Iron-Oxo Species, Environ. Sci. Technol. 52 (2018) 2197–2205.
[16] X. Duan, H. Sun, J. Kang, Y. Wang, S. Indrawirawan, S. Wang, Insights into Heterogeneous Catalysis of Persulfate Activation on Dimensional-Structured Nanocarbons, ACS Catal. 5 (2015) 4629–4636.
[17] X. Cheng, H. Guo, Y. Zhang, X. Wu, Y. Liu, Non-photochemical production of singlet oxygen via activation of persulfate by carbon nanotubes, Water Res. 113 (2017) 80–88.
[18] G.-D. Fang, D.D. Dionysiou, S.R. Al-Abed, D.-M. Zhou, Superoxide radical driving the activation of persulfate by magnetite nanoparticles: Implications for the degradation of PCBs, Appl. Catal. B 129 (2013) 325–332.
[19] A.L. Teel, M. Ahmad, R.J. Watts, Persulfate activation by naturally occurring trace minerals, J. Hazard. Mater. 196 (2011) 153–159.
[20] G. Fang, J. Gao, D.D. Dionysiou, C. Liu, D. Zhou, Activation of persulfate by quinones: free radical reactions and implication for the degradation of PCBs, Environ. Sci. Technol. 47 (2013) 4605–4611.
[21] R.A. Livingston, Influence of the environment on the patina of the Statue of Liberty, Environ. Sci. Technol. 25 (1991) 1400–1408.
[22] E. Kociołek-Balawejder, E. Stanisławska, I. Jacukowicz-Sobala, Hybrid polymers containing brochantite/tenorite obtained using gel type anion exchanger, React. Funct. Polym. 124 (2018) 12–19.
[23] Z. Li, Y. Ding, S. Li, Y. Jiang, Z. Liu, J. Ge, Highly active, stable and self-antimicrobial enzyme catalysts prepared by biomimetic mineralization of copper hydroxysulfate, Nanoscale 8 (2016) 17440–17445.
[24] A.C. Cardiel, K.J. McDonald, K.-S. Choi, Electrochemical growth of copper hydroxy double salt films and their conversion to nanostructured p-type CuO photocathodes, Langmuir 33 (2017) 9262–9270.
[25] X.Z. Xiao, T.T. Dai, J. Guo, J.H. Wu, Flowerlike Brochantite Nanoplate Superstructures for Catalytic Wet Peroxide Oxidation of Congo Red, ACS Applied Nano Materials 2 (2019) 4159–4168.
[26] K. Huang, J. Wang, D. Wu, S. Lin, Copper hydroxyl sulfate as a heterogeneous catalyst for the catalytic wet peroxide oxidation of phenol, RSC Adv. 5 (2015) 8455–8462.
[27] E.T. Yun, J.H. Lee, J. Kim, H.D. Park, J. Lee, Identifying the Nonradical Mechanism in the Peroxymonosulfate Activation Process: Singlet Oxygenation Versus Mediated Electron Transfer, Environ. Sci. Technol. (2018).
[28] H. Wang, W. Guo, B. Liu, Q. Wu, H. Luo, Q. Zhao, Q. Si, F. Sseguya, N. Ren, Edge-nitrogenated biochar for efficient peroxydisulfate activation: An electron transfer mechanism, Water Res. 160 (2019) 405–414.
[29] C. Liang, C.F. Huang, N. Mohanty, R.M. Kurakalva, A rapid spectrophotometric determination of persulfate anion in ISCO, Chemosphere 73 (2008) 1540–1543.
[30] M. Segall, P.J. Lindan, M.a. Probert, C.J. Pickard, P.J. Hasnip, S. Clark, M. Payne, First-principles simulation: ideas, illustrations and the CASTEP code, J. Phys.: Condens. Matter, 14 (2002) 2717.
[31] Y. Wu, X. Chen, Y. Han, D. Yue, X. Cao, Y. Zhao, X. Qian, Highly Efficient Utilization of Nano-Fe(0) Embedded in Mesoporous Carbon for Activation of Peroxydisulfate, Environ. Sci. Technol. (2019).
[32] Y. Yang, G. Banerjee, G.W. Brudvig, J.H. Kim, J.J. Pignatello, Oxidation of Organic Compounds in Water by Unactivated Peroxymonosulfate, Environ. Sci. Technol. (2018).
[33] H. Lee, H.I. Kim, S. Weon, W. Choi, Y.S. Hwang, J. Seo, C. Lee, J.H. Kim, Activation of Persulfates by Graphitized Nanodiamonds for Removal of Organic Compounds, Environ. Sci. Technol. 50 (2016) 10134–10142.
[34] T. Zhang, Y. Chen, Y. Wang, J. Le Roux, Y. Yang, J.P. Croue, Efficient peroxydisulfate activation process not relying on sulfate radical generation for water pollutant degradation, Environ. Sci. Technol. 48 (2014) 5868–5875.
[35] X. Cheng, H. Guo, Y. Zhang, G.V. Korshin, B. Yang, Insights into the mechanism of nonradical reactions of persulfate activated by carbon nanotubes: Activation performance and structure-function relationship, Water Res. (2019).
[36] X. Zhang, Y. Ding, H. Tang, X. Han, L. Zhu, N. Wang, Degradation of bisphenol A by hydrogen peroxide activated with CuFeO 2 microparticles as a heterogeneous Fenton-like catalyst: Efficiency, stability and mechanism, Chem. Eng. J. 236 (2014) 251–262.
[37] R. Zhao, T. Yang, M.A. Miller, C.K. Chan, Electrochemical properties of nanostructured copper hydroxysulfate mineral brochantite upon reaction with lithium, Nano Lett. 13 (2013) 6055–6063.

[38] V. Hayez, A. Franquet, A. Hubin, H. Terryn, XPS study of the atmospheric corrosion of copper alloys of archaeological interest, Surf. Interface Anal. 36 (2004) 876–879.
[39] W. Nie, Q. Mao, Y. Ding, Y. Hu, H. Tang, Highly efficient catalysis of chalcopyrite with surface bonded ferrous species for activation of peroxymonosulfate toward degradation of bisphenol A: A mechanism study, J. Hazard. Mater. 364 (2019) 59–68.
[40] X. Xue, K. Hanna, C. Despas, F. Wu, N. Deng, Effect of chelating agent on the oxidation rate of PCP in the magnetite/H2O2 system at neutral pH, J. Mol. Catal. A: Chem. 311 (2009) 29–35.
[41] W. Jia, E. Reitz, H. Sun, H. Zhang, Y. Lei, Synthesis and characterization of novel nanostructured fishbone-like Cu(OH)2 and CuO from Cu4SO4(OH)6, Mater. Lett. 63 (2009) 519–522.
[42] L. Kong, G. Fang, Y. Chen, M. Xie, F. Zhu, L. Ma, D. Zhou, J. Zhan, Efficient activation of persulfate decomposition by Cu2FeSnS4 nanomaterial for bisphenol A degradation: Kinetics, performance and mechanism studies, Appl. Catal. B 253 (2019) 278–285.
[43] H. Wang, W. Guo, R. Yin, J. Du, Q. Wu, H. Luo, B. Liu, F. Sseguya, N. Ren, Biochar-induced Fe (III) reduction for persulfate activation in sulfamethoxazole degradation: Insight into the electron transfer, radical oxidation and degradation pathways, Chem. Eng. J. 362 (2019) 561–569.